How intimate contact with nanoporous carbon benefits the reversible hydrogen desorption from NaH and $NaAlH_4$†

Philipp Adelhelm, Krijn P. de Jong and Petra E. de Jongh*

Received (in Cambridge, UK) 28th May 2009, Accepted 14th August 2009
First published as an Advance Article on the web 28th August 2009
DOI: 10.1039/b910461e

The kinetics and thermodynamics for the reversible hydrogen desorption from NaH (and NaH derived from $NaAlH_4$) are greatly improved by nanosizing and providing close contact to a porous carbon matrix.

Metal hydrides are promising candidates for compact on-board storage of hydrogen.[1–3] However, no metal hydride system so far meets all requirements, as slow kinetics, high thermodynamic stability of the hydride and/or reversibility issues hamper practical application. It is expected that nanosizing and confining a material can improve the kinetics of the hydrogenation and dehydrogenation reactions, limit phase segregation and particle growth, and might influence the thermodynamic properties of the system.[4–7] Improved kinetics and reversibility were found for nanosized $NaAlH_4$ deposited on carbon nanofibers[8] and mixed with high surface area carbon.[9] Here we discuss how the sorption behavior of NaH and $NaAlH_4$ is influenced by intimate contact with nanoporous carbon. We will show that not only faster kinetics are observed but also a shift in the equilibrium conditions which is at least partly due to reversible interaction between Na and the carbon matrix.

Fig. 1 shows the dehydrogenation behavior of NaH (95%, Aldrich) mixed with high surface area carbon upon heating in Ar atmosphere. The high purity carbon (HSAG-500, Timcal Ltd.) is turbostratic, and exhibits a BET surface area of 500 $m^2\ g^{-1}$, a pore volume of 0.66 $cm^3\ g^{-1}$ and pores mainly in the micro- and mesopore range. The hydrogen desorption is significantly affected by the presence of carbon. Pure NaH shows hydrogen release between 300 and 400 °C. In contrast, the physical mixture of 90 wt% carbon and 10 wt% NaH (10NaH/C) starts to desorb already around 150 °C with the maximum desorption rate at 240 °C. A sample containing 33 wt% NaH (33NaH/C) shows combined behavior, with two desorption peaks. Typically 3.8–4.4 wt% hydrogen with respect to the NaH was evolved, close to the theoretical amount (4.2 wt%).

For 33NaH/C, the pore volume loss upon heating was 0.36 $cm^3\ g\ (C)^{-1}$ for $d < 70$ nm, as determined using nitrogen physisorption (Fig. S1, ESI†). This is less than the volume of Na added (0.48 $cm^3\ g\ (C)^{-1}$). Nevertheless it suggests that upon dehydrogenation of NaH, most of the liquid Na (T_m = 97.8 °C) infiltrates the nanoporous carbon to form nanoconfined solid Na after cooling.

Fig. 2 shows the XRD patterns of the 33NaH/C mixture before (A) and after dehydrogenation under Ar atmosphere (325 °C, 5 h) (B). The XRD pattern of the mixture shows NaH diffraction lines, and two lines at 31° (002) and around 52° (10) 2θ that are typical for turbostratic carbon materials. After dehydrogenation, the XRD pattern shows a broad Na diffraction line at 34.4°, evidencing that the NaH decomposed to form Na nanocrystallites. A volume-averaged crystallite size of 12 nm was estimated from the line broadening using the Scherrer equation. Interestingly, a shift of the carbon (002) diffraction line from 31° to 29.3° is also observed. The shift corresponds to an increase in the average graphene interlayer spacing from 3.35 Å to 3.54 Å, suggesting intercalation of Na between the graphene layers. This value of 3.54 Å is however smaller than the 4.55 Å distance reported in the literature between two sodium-intercalated graphene sheets, which accounts for the formation in the present case of high stage intercalation compounds. This is in line with results found for turbostratic carbons with similar microstructures.[10–12] A change in the interlayer spacing by 0.19 Å indicates that not all sodium is intercalated as also evidenced by the diffraction lines due to metallic sodium. Intercalation is also supported by the decrease in peak intensity, since interlayer species will lead to destructive interference. For sample 10NaH/C, no crystalline sodium and a smaller shift in the (002) diffraction line to 30.4° was observed (data not shown), as expected due to the lower sodium content.

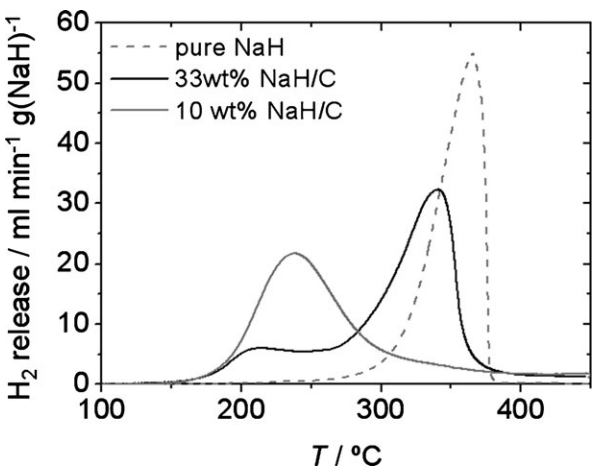

Fig. 1 Thermal programmed desorption (TPD) of NaH after mixing with porous carbon (Ar atmosphere, 5 K min^{-1}). The desorption profiles are normalized per gram of NaH.

Inorganic Chemistry and Catalysis, Debye Institute for Nanomaterials Science, Utrecht University, Sorbonnelaan 16, 3584 CA Utrecht, The Netherlands. E-mail: p.e.dejongh@uu.nl; Fax: +31 30 251 1027; Tel: +31 30 253 7400

† Electronic supplementary information (ESI) available: Porosity measurements, dehydrogenation behavior of LiH/carbon composite, cycling of 33NaH/C under H_2 atmosphere, experimental details. See DOI: 10.1039/b910461e

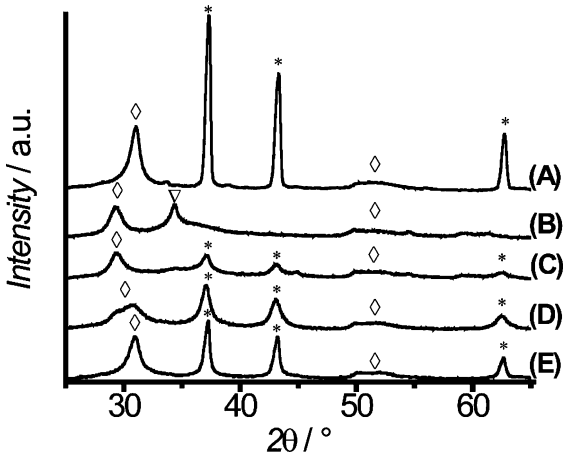

Fig. 2 XRD patterns of samples containing 33 wt% NaH on carbon (33NaH/C). (A) Physical mixture for comparison, (B) after dehydrogenation under Ar (325 °C, 5 h), (C) and (D) after rehydrogenation at room temperature under 1 bar H_2 (for 1 h) and 50 bar H_2 (for 10 h), (E) after cyclic treatment under H_2 atmosphere between 50 and 380 °C (ended in hydrogenated state, 4 cycles). ◇ = carbon, * = NaH, ▽ = Na.

The intercalation of Li and K into graphite has been extensively studied as a means to increase the *physisorption* of H_2. The only intercalation compounds for which H *chemisorption* has been reported are C_8KH_x, and C_8RbH_x in which the H atoms are sandwiched between the intercalated alkali metal atoms, leading to large interlayer distances.[13] Na does not intercalate as easily as other alkali metals. Although intercalation of a limited amount of Na between the graphene sheets in both well-defined graphite and turbostratic carbon has been reported before,[14–16] as far as we are aware no studies exist on the reversible H_2 interaction with these compounds. Preliminary measurements on LiH/C mixtures showed that also in this case H_2 release at low temperatures is observed, however lithium carbide (Li_2C_2) is formed at high temperatures (Fig. S2, ESI†).

Rehydrogenation of Na was found to start already under very mild conditions. The NaH diffraction lines reappeared after exposing the sample to hydrogen atmosphere (1 bar) at room temperature for one hour (curve C). A higher degree of hydrogenation was obtained with increased pressure (50 bar) and hydrogenation time (10 h, curve D). The broad feature around $2\theta = 30°$ could correspond to the presence of both intercalated and deintercalated graphene stacks. Around 40% of the theoretical hydrogen content of NaH could be released after rehydrogenation at 1 bar (50% after rehydrogenation at 50 bar H_2) as determined by TPD. The NaH crystallite size after rehydrogenation was 10–17 nm using the Scherrer equation, evidencing that the nanosize was preserved during rehydrogenation.

For bulk NaH the dehydrogenation enthalpy is 56 kJ mol $(NaH)^{-1}$, corresponding to an equilibrium pressure of 1 bar H_2 at temperatures of 400–450 °C.[17–20] Our 33NaH/C mixture was first dehydrogenated under Ar flow and then cycled under 1 bar H_2 between 50 and 380 °C (5 K min^{-1}) using a magnetic suspension balance. Remarkably, partial decomposition under 1 bar H_2 started already at 225 °C (Fig. S3, ESI†). 20% of the theoretical amount of hydrogen was released when heating to 380 °C (so well below the bulk equilibrium decomposition temperature). The XRD pattern of the hydrogenated sample after 4 cycles is shown in Fig. 2 (curve E) and illustrates the reversibility of the process. Typically, dehydrogenation of NaH is not considered relevant, as it occurs at high temperatures due to the high thermodynamic stability of the hydride with respect to metallic Na. However, we clearly measure a lower dehydrogenation enthalpy than for bulk NaH. This can at least partly be attributed to the fact that the metallic phase is now stabilized by intercalation. Intercalation energies for Na in carbon have not been reported, but for light alkali metals such as Li and K, they are in the order of 10–30 kJ mol $(metal)^{-1}$.[21] For a 33 wt% NaH mixture with a non-porous, graphitic, material a significantly smaller part of the NaH releases hydrogen starting at 225 °C (Fig. S3, ESI†), while also Na is intercalated to a lesser extent according to XRD (not shown), supporting the fact that the destabilization of NaH is directly related to the intercalation of the Na. However, it cannot be excluded that also nanosizing plays a role; it is theoretically predicted that the stability of NaH decreases for sizes smaller than 2 nm.[7]

Modification of the hydrogen sorption properties of NaH is in particular interesting for the $NaAlH_4$ system. After the discovery of Ti as an effective catalyst,[22] the $NaAlH_4$ system gained a lot of attention as it is one of the few systems with thermodynamics that could allow operation at PEM fuel cell operating temperatures. Decomposition of $NaAlH_4$ to NaH, Al and H_2 yields 5.55 wt% hydrogen.[23] Another 1.85 wt% could be obtained by decomposition of NaH, however this step is usually not considered due to the high stability of the hydride. (Note: $NaAlH_4$ decomposes in three steps upon heating: $NaAlH_4 \rightarrow 1/3Na_3AlH_6 + 2/3Al + H_2$; $Na_3AlH_6 \rightarrow 3NaH + Al + 3/2H_2$; $NaH \rightarrow Na + 1/2H_2$.) Decreasing the stability of NaH could thus offer a way to yield the full 7.4 wt% hydrogen from $NaAlH_4$. It is hence worth studying what the effect of porous carbon is on the overall hydrogen sorption properties of $NaAlH_4$.

Fig. 3a shows the desorption profile under Ar of both a 40 wt% $NaAlH_4$/carbon mixture ($40NaAlH_4$/C) and pure $NaAlH_4$. As expected, pure $NaAlH_4$ (>90%, Aldrich) decomposes in several steps, starting from its melting point around 180 °C. Decomposition of NaH derived from pure $NaAlH_4$ occurs well above 300 °C with the maximum at around 370 °C, in good agreement with the results for pure NaH shown in Fig. 1. Compared to pure $NaAlH_4$, $40NaAlH_4$/C shows a markedly improved dehydrogenation behavior. Hydrogen release already starts at 170 °C. Most of the hydrogen desorbs in a relatively small temperature range up to 230 °C. At 218 °C already 5.55 wt% hydrogen is released, which nominally corresponds to decomposition of $NaAlH_4$ to NaH (which would result in 23 wt% NaH on carbon). As further continuous release of hydrogen takes place, it is clear that part of the $NaAlH_4$ has fully decomposed to Na at temperatures well below 250 °C. Some further hydrogen release at 306 °C is in agreement with the results found for the decomposition of the NaH–carbon mixtures shown in Fig. 1. Fig. 3b shows the XRD patterns of the $40NaAlH_4$/C mixture (A), after dehydrogenation under Ar atmosphere

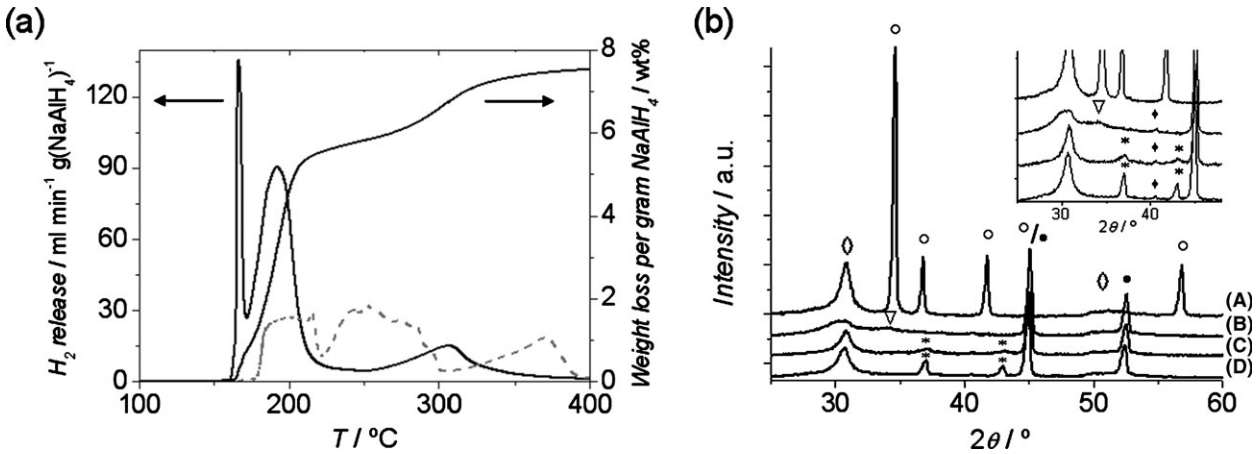

Fig. 3 (a) Thermal programmed desorption of a 40 wt% $NaAlH_4$/carbon mixture ($40NaAlH_4$/C) and corresponding weight loss in wt% (solid lines) under Ar atmosphere (25 ml min^{-1}, 5 K min^{-1}). Pure $NaAlH_4$ is added for comparison (dashed line), (b) XRD patterns of $40NaAlH_4$/C (A) before and (B) after dehydrogenation under Ar atmosphere (325 °C, 5 h), (C) after rehydrogenation at room temperature under 50 bar H_2 pressure for 10 h and (D) after cyclic treatment between 50 and 380 °C (ended in hydrogenated state, 4 cycles). ◇: carbon, °: $NaAlH_4$, ▽: Na, ●: Al, ◆: Al (K_β), *: NaH.

(325 °C, 5 h) (B), and after rehydrogenation at room temperature (50 bar H_2, 10 h) and cycling (C–D). Even though the diffraction lines are less distinct, the features of the carbon, Na and NaH diffraction lines are similar to what was found for the 33NaH/C samples shown in Fig. 2, hence partial rehydrogenation at room temperature is found.

In summary, the hydrogen sorption properties of NaH and $NaAlH_4$ can be markedly improved by the presence of nanoporous carbon. Upon dehydrogenation, melt infiltration of the carbon results in nanocomposite materials, with metal (hydride) confined in the pores of the carbon. Hydrogen release temperatures are drastically reduced compared to the pure compounds, even under 1 bar H_2 pressure, and partial rehydrogenation occurs under mild conditions even at room temperature. Reversible intercalation of Na in between the graphene sheets causes a favorable shift in the (de)hydrogenation equilibrium conditions. The results are very relevant for $NaAlH_4$ as a hydrogen storage material, as the destabilization of NaH relative to the (intercalated) metal phase promotes the full decomposition of $NaAlH_4$ into its elements, yielding an extra 1.85 wt% hydrogen at reduced temperatures.

We would like to thank Timcal Ltd., Bodio, Switzerland, for providing the porous carbon material. We acknowledge NWO-ACTS and a NWO-Vidi grant (016.072.316) for financial support.

Notes and references

1 L. Schlapbach and A. Zuttel, *Nature*, 2001, **414**, 353–358.
2 S. I. Orimo, Y. Nakamori, J. R. Eliseo, A. Zuttel and C. M. Jensen, *Chem. Rev.*, 2007, **107**, 4111.
3 B. Sakintuna, F. Lamari-Darkrim and M. Hirscher, *Int. J. Hydrogen Energy*, 2007, **32**, 1121.
4 R. W. P. Wagemans, J. H. van Lenthe, P. E. de Jongh, A. J. van Dillen and K. P. de Jong, *J. Am. Chem. Soc.*, 2005, **127**, 16675–16680.
5 S. Cheung, W. Q. Deng, A. C. T. van Duin and W. A. Goddard, *J. Phys. Chem. A*, 2005, **109**, 851–859.
6 V. Berube, G. Radtke, M. Dresselhaus and G. Chen, *Int. J. Energy Res.*, 2007, **31**, 637–663.
7 J. G. O. Ojwang, R. van Santen, G. J. Kramer, A. C. T. van Duin and W. A. Goddard, *J. Chem. Phys.*, 2008, **128**, 164714.
8 C. P. Baldé, B. P. C. Hereijgers, J. H. Bitter and K. P. de Jong, *J. Am. Chem. Soc.*, 2008, **130**, 6761–6765.
9 C. Cento, P. Gislon, M. Bilgili, A. Masci, Q. Zheng and P. P. Prosini, *J. Alloys Compd.*, 2007, **437**, 360–366.
10 C. Sechet, D. Sarmeo, M. Mermoux, P. Touzain, L. Bonnetain, D. Dumas, B. Allard and R. Paulus, *Mol. Cryst. Liq. Cryst.*, 1994, **245**, 153–158.
11 L. Joncourt, M. Mermoux, P. Touzain, L. Bonnetain, D. Dumas and B. Allard, *J. Phys. Chem. Solids*, 1996, **57**, 877–882.
12 *Chemistry and Physics of Carbon*, ed. P. A. Thrower and P. L. Walker, Dekker, New York, vol. 10—p. 142, vol. 45—p. 1, vol. 20—p. 213.
13 T. Enoki, S. Miyajima, M. Sano and H. Inokuchi, *J. Mater. Res.*, 1990, **5**, 435–466, and references therein.
14 D. A. Stevens and J. R. Dahn, *J. Electrochem. Soc.*, 2001, **148**, A803.
15 N. Akuzawa, J. Yoshioka, C. Ozaki, M. Tokuda, K. Ohkura and Y. Soneda, *Mol. Cryst. Liq. Cryst. Sci. Technol., Sect. A*, 2002, **388**, 415–421.
16 S. Pruvost, C. Herold, A. Herold and P. Lagrange, *Carbon*, 2004, **42**, 1825–1831.
17 J. Subrt and K. Tobola, *J. Therm. Anal. Calorim.*, 1976, **10**, 5–12.
18 X. Z. Ke and I. Tanaka, *Phys. Rev. B*, 2005, **71**, 024117.
19 A. F. Holleman, E. Wiberg and N. Wiberg, *Lehrbuch der Anorganischen Chemie*, W. de Gruyter, Berlin, 2007, p. 1279.
20 HSC Chemistry Ver. 4.1., Outokumpu Research Oy, Pori, Finland.
21 V. V. Avdeev, A. P. Savchenkova, L. A. Monyakina, I. V. Nikolskaya and A. V. Khvostov, *J. Phys. Chem. Solids*, 1996, **57**, 947–949.
22 B. Bogdanovic and M. Schwickardi, *J. Alloys Compd.*, 1997, **253**, 1–9.
23 B. Bogdanovic, R. A. Brand, A. Marjanovic, M. Schwickardi and J. Tölle, *J. Alloys Compd.*, 2000, **302**, 36–58.